LICORNE a benchmark on numerical method for non-linear site response analysis involving pore water pressure

Christina Khalil, Julie Régnier, Fernando Lopez-caballero

3rd EUROPEAN CONFERENCE ON
EARTHQUAKE ENGINEERING & SEISMOLOGY
BUCHAREST, ROMANIA, 2022

LICORNE a benchmark on numerical method for non-linear site response analysis involving pore water pressure

Christina Khalil – École Supérieur d'Ingénieurs des Travaux de la Construction (ESITC Paris), Arcueil, France, khalil@esitc-paris.fr

Julie Régnier – Cerema research team REPSODY, Sophia-Antipolis, France, julie.regnier@cerema.fr

Fernando Lopez-Caballero –Laboratoire de Mécanique Paris-Saclay (LMPS) CNRS UMR-9026, Université Paris Saclay, CentraleSupélec, École Normale Supérieure, Gif-sur-Yvette, France, fernando.lopez-caballero@centralesupelec.fr

And the LICORNE participants : Vinicius Alves-Fernandes (EDF), Anna Chiaradonna (UnivAQ), Reine Fares (CEA), Evelyne Foerster (CEA), Stefania Gobbi (GDS), Cyril Gomes (Fugro), Emmanuel Javelaud (EDF), Ziad Kteich (Tractbel), Silvana Montoya-Noguera (EAFIT), Elif Oral (Geoazur, Caltech), Maria-Paola Santisi d'Avila (UCA)

Abstract: Following the benchmark PRENOLIN for 1D non-linear site response analysis a new benchmark is proposed to assess the effect of both, the pore water pressure generation and the liquefaction occurrence. For now, 11 teams, mainly from French institutes, participate in this benchmark. A first iteration of calculation based on a synthetic case has been performed and a second is ongoing. The first iteration of the LICORNE (**L**iquefaction and **C**yclic m**O**bility **R**epresentation on **N**umerical **E**xperiments) project highlighted differences in the results of some numerical codes. In parallel, other codes were able to closely estimate the responses. A second iteration is ongoing to clarify the inputs and the results form of each team and propose additional tests to analyse in more detail the stress-strain curves produced by each team.

Keywords: site response analysis, non-linear, pore water pressure, liquefaction

1. Introduction

The seismic amplification associated with the subsurface soil layers has demonstrated their destructive potential. During strong to moderate earthquakes, the seismic wave propagation in the soft soil layers can induce large strains and trigger strong non-linearity in the soil behaviour impacting significantly the site response (Régnier et al. 2013). In the presence of saturated, poorly compacted and non-cohesive materials, the seismic loading coupled with medium to large strain amplitude can produce excess pore water pressure. If the pore pressure excess reaches large values, soil failure with liquefaction phenomenon occurs. In such case, soil has no longer the strength to support static stresses, thus large vertical and lateral permanent displacements can occur (Seed and Idriss 1971). The problem should no longer be solved with a single-phase model, but with a fluid-solid two-phase model.

In current practice, site response analysis are performed using 1-D numerical simulations with either equivalent linear approaches or more advanced non-linear constitutive models. In the former, the soil behavior is characterized by the shear modulus reduction and the increase of attenuation curves. In the latter, it is necessary to have more parameters dueto the complexity of these models. In the PRENOLIN project (2012-2015), the uncertainties of the non-linear site response estimation, linked to the soil model and code were calculated. One main limitation of this project was the non-consideration of the pore pressure development. The Benchmark LICORNE (**L**iquefaction and **C**yclic m**O**bility **R**epresentation on **N**umerical **E**xperiments) goes one step further with the comparison of numerical evaluation of 1D non-linear site response involving pore water pressure generation. Eleven teams participate with different numerical codes in this international benchmark. The submitted results of each team were compared all together. As most of

databases issued from *in-situ* measurements or centrifuge tests, among others, are not fully complete in terms of soil mechanic properties and/or the range of deformations, it was decided to use as a reference database, numerical simulations based on a fully non-linear constitutive model. Thus, the soil parameters and the reference data were inspired by the PhD thesis of Khalil (2021).

The objective of this paper is to present the benchmark database, the numerical models used by the participants, the preliminary results of the first iteration, and the perspectives for a second iteration of calculations.

2. Presentation of the participants

For the LICORNE benchmark, 11 teams participated and are presented in Table 1. They are mainly from French public institutions (UCA, Cerema, Geoazur, CEA), French companies (GDS, EDF, Fugro, Tractebel/Engie), one institution in Colombia (EAFIT) and one in Italy (UnivAQ).

The reference calculations were conducted with the finite element code GEFDyn (Aubry et al. 1986; Aubry and Modaressi 1996), and the reference soil constitutive model was the ECP (Ecole Centrale Paris) elastoplastic multi-mechanism model, also known as Hujeux model (Aubry et al. 1982). The reason behind this choice is that this model can take into account the soil behaviour for a large range of deformations. Moreover, it is interesting to mention that some participants share the same FE code (i.e. Team G) or the soil model (i.e. Teams F, G and I) as the reference. This added a challenge in the project to verify the uncertainties of each code/model and their ability to represent the non-linear soil behaviour or the liquefaction apparition.

Table 1 : Participating teams to benchmark LICORNE

ID	Numerical code	Numerical method	Constitutive model	References
A	SWAP_3C	Quadratic line finite elements with 3 nodes	IWAN + IAI	(Santisi d'Avila et al. 2018)
B	SEM2DPACK	Spectral element method	IWAN + IAI	(Oral, Gélis, and Bonilla 2019; Oral 2016)
C	OPENSEES	Finite element, 9_4_QuadUP elements	Pressure dependent MultiYield	(Prevost 1985; Parra-Colmenares 1996; Yang and Elgamal 2000; Elgamal et al. 2003)
D	Code_Aster	FEM	Extended Equivalent Linear	(Kteich et al. 2019)
F	CyberQuake	FEM	Hujeux	(Hujeux 1985; Modaressi and Foerster 2000; Lopez-Caballero et al 2007);
G	GEFDyn	FEM	Hujeux	Aubry et al. 1982; Aubry and Modaressi 1996
H	DEEPSOIL	Finite difference method	Extended hyperbolic model	(Hashash 2016)
I	code_aster	FEM	Hujeux	(Aubry et al. 1982; "code_aster" 2021)
K	EERA	FEM	Extended Equivalent Linear	(Kteich et al. 2019)
L1	SCOSSA PWP B1.91	FEM	Modified Hyperbolic model (MKZ + PWP model) With pwp dissipation	(Chiaradonna et al. 2018; 2020; Tropeano et al. 2019)
L2	SCOSSA PWP B1.91	FEM	Modified Hyperbolic model (MKZ + PWP model) With pwp dissipation	
L3	SCOSSA PWP B1.91	FEM	Modified Hyperbolic model (MKZ + PWP model) With pwp dissipation/ CTX	
M	OPENSEES	FEM	Manzari-Dafalias (2004)	(Dafalias and Manzari 2004)

3. Presentation of the calculation case

3.1. Soil layer geometry and properties

The soil profile named P1 (**Figure 1**) is composed of two layers: 6 m dense sand (Mat.1 Sand) below a 4 m loose sand (Mat.2 Sand). The water table is 1 m below the surface.

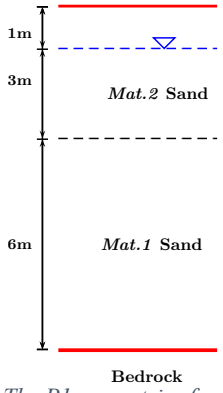

Figure 1: The P1 geometries for iteration 1

Considering the sign convention of soil mechanics that considers the compression as positive, some soil layer properties are set in Table 2.

Table 2 : Soil layer properties

	Dense sand - mat1	Loose sand - mat2
Solid Density ρ_s $[kg/m^3]$	2700	2700
Poisson's ratio υ [1]	0.28	0.3
Porosity [1]	0.35	0.35
Shear Modulus G_{ref} [MPa]	719.5	290
Non linear degree n_e [1]	0.47	0.5
Reference mean stress p'_{ref} [MPa]	1	1
Permeability k_h $[m/s]$	10^{-5}	10^{-4}
Permeability k_v $[m/s]$	10^{-5}	10^{-4}

As a mandatory step to identify soil type and behaviour, simulated triaxial drained/undrained tests were conducted on each soil sample. For the sake of brevity only, the simulated laboratory tests results will not be presented in this paper. On the contrary, the obtained curves of the cyclic stress ratio (SR = $\frac{\boldsymbol{\sigma_{v,cyc}}}{\mathbf{2p'_0}}$, with $\boldsymbol{\sigma_{v,cyc}}$ is the cyclic vertical stress applied in the cyclic loading and p'_0 mean effective stress) as a function of the number of cycles to produce liquefaction (N), are shown in **Figure 2** (a). As a comparison with the experimentally obtained curves given by Byrne et al. (2004) for Nevada sand at different densities, it can be seen from **Figure 2** (a) that the shallow soil layer has a relative density close to 40%, which makes it behave as a loose sand and thus has a tendency to liquefy. Whereas the deep soil is a dense sand of a relative density close to 70%.

In addition, the $\boldsymbol{G/G_{max} - \gamma}$ curves are given in **Figure 2** (b). As a qualitative comparison, the modelled test results are compared with the reference curves given by Seed and Idriss (1971).

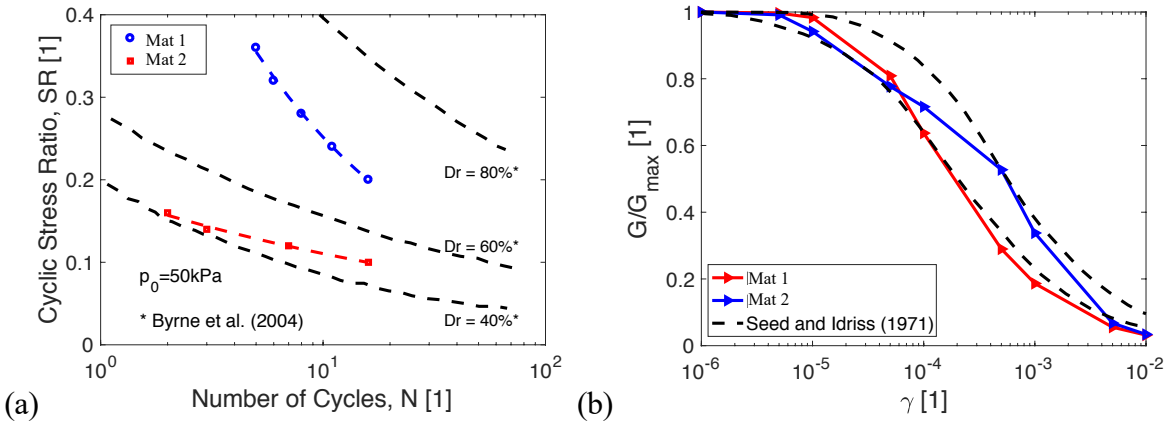

Figure 2: The soil layers behavior: (a) Cyclic stress ratios against the number of cycles and (b) normalized Shear modulus reduction curves.

3.2 Input ground motions

Input motions with different high frequency and low frequency content time series are tested (so-called Ts hf and Ts lf). The motions are enumerated from 0 to 3 meaning that 0 is the low motion and 3 is the strong motion. The outcropping bedrock motion is inserted through the bottom of the model as incident waves after deconvolution. These accelerations are filtered for frequencies between 0.15 and 30 Hz. The final PGA of the given input motions and their Fourier spectra are presented in **Figure 3**.

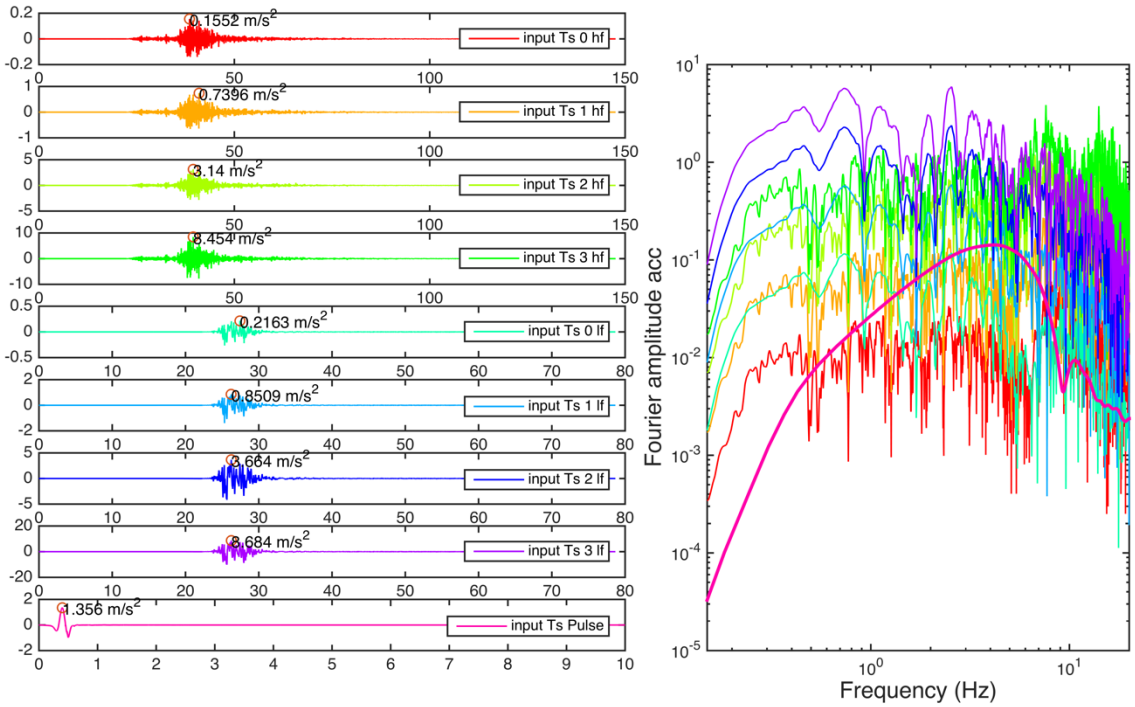

Figure 3 : Acceleration time histories (left) and associated Fourier spectra of the input motions (right) for profile P1.

2. Results

The participants were asked to provide the following data:

- the stress strain curve every 1m from the surface
- the vertical settlement at the top of the column
- the acceleration time history at the top of the column
- the temporal change of the excess pore water pressure ratio ($r_u = \frac{\Delta p_w}{p'_0}$; Δp_w being the difference between the final and initial pore water pressure and the p'_0 is the initial mean effective stress) every 1m from the surface (for column P1 only)

For the sake of brevity only, not all the results are shown in this paper, only some results will be developed hereafter.

The ratio of Fourier spectra between the surface motion and the input was calculated and is shown in **Figure 4** for all motions. The Fourier spectra were calculated using the fast Fourier Transform algorithm after applying a baseline correction followed by an apodisation on 2% of the signal. The spectra were smoothed with a Konno-Ohmachi smoothing (Konno & Ohmachi, 1998) with a parameter b = 40. The resonance frequency decreases between the simulations performed with the weakest motion (Ts0) and the strongest motion (Ts3). In addition, except for the results of the linear equivalent analysis, the shape of the linear transfer function disappears from the Ts2 level. From this acceleration level it is observed that, for all the calculations (except teams B and D), the ratio is below 1 (i.e. de-amplification) on the majority of the frequency band.

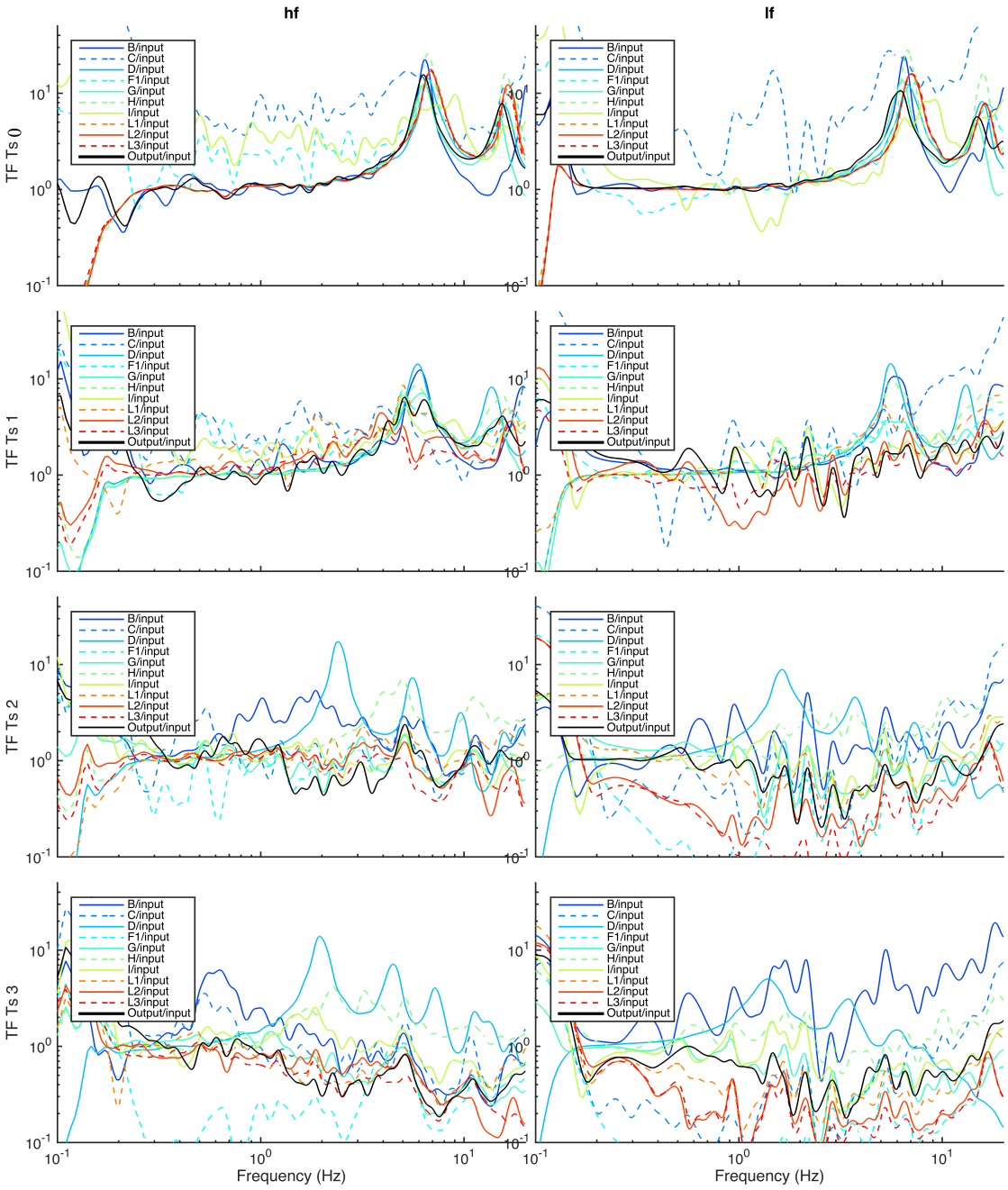

Figure 4 : Fourier spectral ratio of the HF (left column) and LF (right column) for the fourth levels of input motion, from the weakest at the top to the strongest at the bottom.

Ru_{max} profiles are shown in **Figure 5**, for the pulse seismic motion and the highest amplitude motions (Ts2 and Ts3). When the excess pore water pressure ratio, r_u, is greater than 0.8, liquefaction occurs. Hence, it can be seen, from the results of **Figure 5**, that some codes were able to detect liquefaction in the first layer (as expected due to the type of sand of this layer). However, for the strongest input motions, some codes (Teams B and C) detected a liquefaction occurrence in the dense sand where it is not supposed to liquefy. These results may notify some numerical problems that will be further analyzed in the next step of calculations.

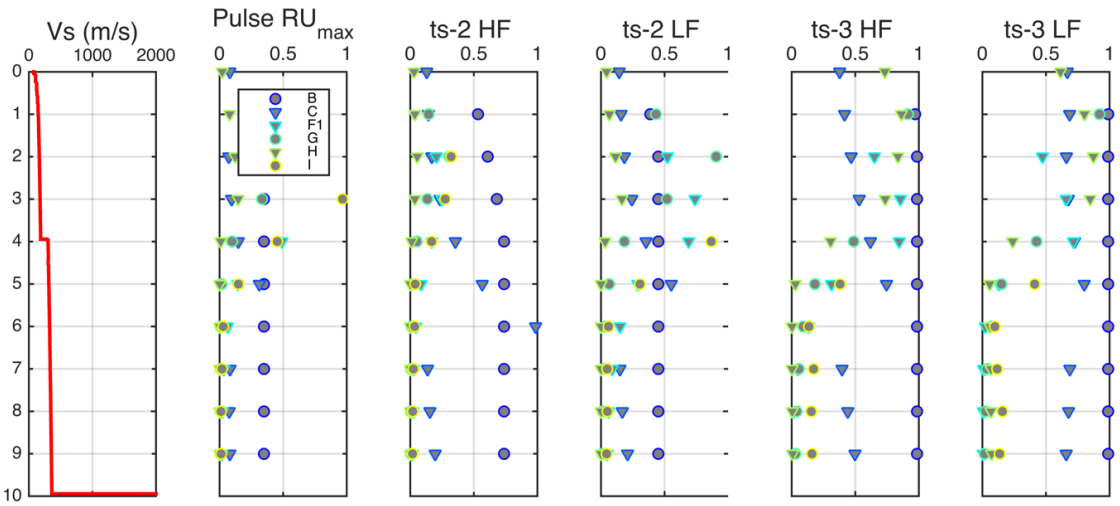

Figure 5: Rumax profiles for the pulse, the motions HF and LF scaled to the two strongest levels.

The variability between the codes has been calculated for seven parameters and for all the input motions (**Figure 6**): the PGA at the surface, the spectral acceleration at 0.1s, 0.3 s and 1 s and the maximum pore water pressure ratio, shear stress and shear strain at 3.5m (Z3). The variability is larger for the maximum shear strain. It increases with the level of input motion for the spectral values but decreases for the maximum pore water pressure ratio.

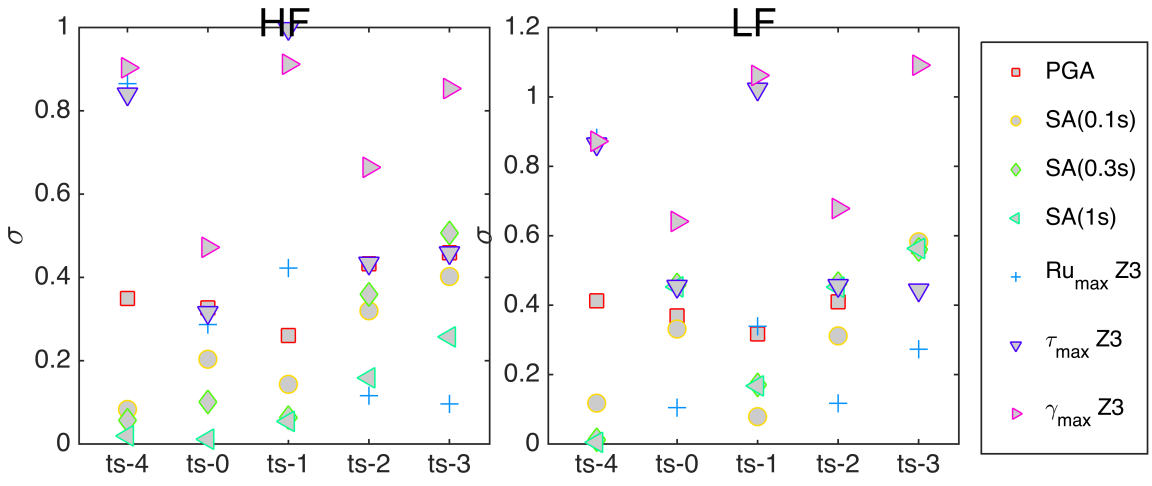

Figure 6 : Variability between codes for seven parameters: the PGA at the surface, the spectral acceleration(SA) at 0.1s, 0.3 s and 1 s, the maximal pore water pressure ratio (Ru), shear stress and shear strain at 3.5m (Z3) for all input motions.

2. Conclusions

This first round of calculations has demonstrated a large variability between the participants' results. For weak motions (Ts0), the site response variability indicated that some calculations could be improved. In addition, some incoherent results appear for some codes. For example, at larger strain, these codes found a liquefaction occurrence in the second soil layer which is not likely to occur due to the soil type. Moreover, the variability of the spectral parameters and the maximum shear strains increase which may reflect some differences resulting from the constitutive models of the participants.
Thus, for the second round of calculations, the organizing committee plans that the given data were well incorporated by each team, and that the teams with outlier results will perform additional verification. Another important aspect of the second iteration is that it will be possible to understand whether the differences originate from the model predictions or simulation setup mistakes in the implementations/calibrations of the data, the second round of benchmark will include an additional case study that will allow for the comparison between the stress-strain curves of each team. The preliminary analysis of the results will be extended with the calculation of Anderson criteria and new parameters such as the cumulative damage Q factor (Shinozuka and Ohtomo 1989).

Acknowledgements

The authors would like to thank to the French permanent accelerometric network (RAP/RESIF) that funded the working group γ-G that initiated this benchmark.

References

Aubry, D., D. Chouvet, A. Modaressi, and H. Modaressi. 1986. "GEFDYN: Logiciel d'analyse de Comportement Mécanique Des Sols Par Éléments Finis Avec Prise En Compte Du Couplage Sol-Eau-Air." *Manuel Scientifique, Ecole Centrale Paris, LMSS-Mat*.

Aubry, D., J. C. Hujeux, F. Lassoudiere, and Y. Meimon. 1982. "A Double Memory Model with Multiple Mechanisms for Cyclic Soil Behaviour." In *Proceedings of the Int. Symp. Num. Mod. Geomech*, 3–13.

Aubry, D., and A. Modaressi. 1996. "GEFDYN, Manuel Scientifique." *École Centrale Paris: LMSS-Mat*.

Byrne, Peter M., Sung-Sik Park, Michael Beaty, Michael Sharp, Lenart Gonzalez, and Tarek Abdoun. 2004. "Numerical Modeling of Liquefaction and Comparison with Centrifuge Tests." *Canadian Geotechnical Journal* 41 (2): 193–211.

Chiaradonna, Anna, Alessandro Flora, Anna d'Onofrio, and Emilio Bilotta. 2020. "A Pore Water Pressure Model Calibration Based on In-Situ Test Results." *Soils and Foundations* 60 (2): 327–41.

Chiaradonna, Anna, Giuseppe Tropeano, Anna d'Onofrio, and Francesco Silvestri. 2018. "Development of a Simplified Model for Pore Water Pressure Build-up Induced by Cyclic Loading." *Bulletin of Earthquake Engineering* 16 (9): 3627–52.

"Code_aster. General Public Licensed Structural Mechanics Finite Element Software, Included in the Salomé-Méca Simulation Platform." 2021. R7.01.23. http://www.code-aster.org. - code_aster Reference Constitutive law with cyclical behavior for soil Hujeux.

Dafalias, Yannis F., and Majid T. Manzari. 2004. "Simple Plasticity Sand Model Accounting for Fabric Change Effects." *Journal of Engineering Mechanics* 130 (6): 622–34.

Elgamal, Ahmed, Zhaohui Yang, Ender Parra, and Ahmed Ragheb. 2003. "Modeling of Cyclic Mobility in Saturated Cohesionless Soils." *International Journal of Plasticity* 19 (6): 883–905. http://dx.doi.org/10.1016/S0749-6419(02)00010-4.

Hashash, Youssef MA. 2016. "Nonlinear and Equivalent Linear Seismic Site Response of One-Dimensional Soil Columns." *User Manual v7. 0, Deepsoil Software*.

Hujeux, JC. 1985. "Une Loi de Comportement Pour Le Chargement Cyclique Des Sols." *Génie Parasismique*, 278–302.

Khalil, Christina. 2021. *Seismic Analysis of a Liquefiable Soil Foundation-Embankment System: Life Cycle Performance and Mitigation*. Université Paris-Saclay.

Kteich, Ziad, Pierre Labbé, Emmanuel Javelaud, Jean-François Semblat, and Abdelkrim Bennabi. 2019. "Extended Equivalent Linear Model (X-ELM) to Assess Liquefaction Triggering: Application to the City of

Urayasu during the 2011 Tohoku Earthquake." *Soils and Foundations* 59 (3): 750–63.
Lopez-Caballero, Fernando, Arezou Modaressi-Farahmand Razavi, and Hormoz Modaressi. 2007. "Nonlinear Numerical Method for Earthquake Site Response Analysis I—Elastoplastic Cyclic Model and Parameter Identification Strategy." *Bulletin of Earthquake Engineering* 5 (3): 303–23.
Modaressi, H., and E. Foerster. 2000. "CyberQuake." *User's Manual, BRGM, France*.
Oral, Elif. 2016. "Modélisation Multi-Dimensionnelle de La Propagation Des Ondes Sismiques Dans Des Milieux Linéaires et Non-Linéaires." Paris Est.
Oral, Elif, Céline Gélis, and Luis Fabián Bonilla. 2019. "2-D P-SV and SH Spectral Element Modelling of Seismic Wave Propagation in Non-Linear Media with Pore-Pressure Effects." *Geophysical Journal International* 217 (2): 1353–65.
Parra-Colmenares, Ender Jose. 1996. "Numerical Modeling of Liquefaction and Lateral Ground Deformation Including Cyclic Mobility and Dilation Response in Soil Systems." [Sl: sn].
Prevost, Jean H. 1985. "A Simple Plasticity Theory for Frictional Cohesionless Soils." *International Journal of Soil Dynamics and Earthquake Engineering* 4 (1): 9–17.
Régnier, Julie, Héloïse Cadet, Luis Fabian Bonilla, Etienne Bertrand, and Jean-François Semblat. 2013. "Assessing Nonlinear Behavior of Soils in Seismic Site Response: Statistical Analysis on KiK-net Strong-Motion Data." *Bulletin of the Seismological Society of America* 103 (3): 1750–70.
Santisi d'Avila, Maria Paola, Viet Anh Pham, Luca Lenti, and Jean-François Semblat. 2018. "Extended Iwan-Iai (3DXii) Constitutive Model for 1-Directional 3-Component Seismic Waves in Liquefiable Soils: Applicationto the Kushiro Site (Japan)." *Geophysical Journal International* 215 (1): 252–66.
Seed, Harry Bolton, and Izzat M. Idriss. 1971. "Simplified Procedure for Evaluating Soil Liquefaction Potential." *Journal of Soil Mechanics & Foundations Div*.
Shinozuka, M., and K. Ohtomo. 1989. "Spatial Severity of Liquefaction." In *Proceedings of the Second US-Japan Workshop in Liquefaction, Large Ground Deformation and Their Effects on Lifelines*, 193–206.
Tropeano, Giuseppe, Anna Chiaradonna, Anna d'Onofrio, and Francesco Silvestri. 2019. "A Numerical Model for Non-Linear Coupled Analysis of the Seismic Response of Liquefiable Soils." *Computers and Geotechnics* 105: 211–27.
Yang, Zhaohui, and Ahmed-Waeil Metwalli Elgamal. 2000. *Numerical Modeling of Earthquake Site Response Including Dilation and Liquefaction*. 1. University of California at San Diego, Dept. of Structural Engineering.